Available online at www.sciencedirect.com
ScienceDirect
Applied Clay Science 37 (2007) 157–166
Applied CLAY Science
www.elsevier.com/locate/clay

Rheological behaviour of kaolin/talc/alumina suspensions for manufacturing cordierite foams

João B. Rodrigues Neto [a], Rodrigo Moreno [b,*]

[a] *Sociedade Educacional de Santa Catarina, Albano Schmidt, 3333, 89227-700 Joinville, Brasil*
[b] *Instituto de Cerámica y Vidrio, CSIC, c/ Kelsen n° 5, Cantoblanco 28049 Madrid, Spain*

Received 22 June 2006; received in revised form 5 December 2006; accepted 12 December 2006
Available online 20 December 2006

Abstract

This paper deals with the preparation and rheological characterization of concentrated suspensions (40 vol.% solids) of mixtures of kaolin/talc/alumina to relative weight contents of 40/43.8/16.2, respectively. These concentrated suspensions were thixotropic and viscous, the rheological properties being largely influenced by a number of processing parameters, the most relevant being the nature and content of deflocculant and the pH value. Best results were obtained for a polyacrylic-based polyelectrolyte and pH 11. Green densities of 59% of TD were obtained. Dynamic and static sintering studies were performed and the analysis of the resulting phases was made by XRD. From these tests it was concluded that cordierite phase needed a thermal treatment of 1300 °C to be formed. The sintered slip cast materials have a large residual porosity because of the coarse particle size of the raw materials. Macroporous cordierite foams are obtained by impregnation of polyurethane foam into the optimized slip and heating at 1350 °C/1 h with a burning out step at 550 °C/30 min.

Keywords: Cordierite; Suspensions; Talc; Kaolin; Rheology

1. Introduction

Cordierite, whose composition is $2MgO{\cdot}2Al_2O_3{\cdot}5SiO_2$, is one of the most interesting phases of the system $MgO–SiO_2–Al_2O_3$. Cordierite ceramics have low thermal expansion coefficient, excellent thermal shock resistance, low dielectric constant, and high chemical and mechanical durability. Therefore, cordierite-based materials are extensively used in a broad range of applications, including honeycomb catalysts, integrated circuit boards, and refractories (Mussler and Shafer, 1984; Knickerbocker et al., 1993; Gónzalez-Velasco et al., 1999; Yalamaç and Akkurt, 2006).

The most common method to synthesize cordierite is the high temperature reaction in the solid state, although chemical methods, such as coprecipitation reactions, solution combustion or sol–gel technology have been proposed in order to decrease the synthesis temperature and to improve the physical properties (Awano et al., 1992; Chandran and Patil, 1993; Bertran et al., 2000). Among these methods, sintering of oxide powders through solid state reactions or crystallization of glass powders is the most popular.

* Corresponding author. Tel.: +34 917355840; fax: +34 917355843.
E-mail address: rmoreno@icv.csic.es (R. Moreno).

0169-1317/$ - see front matter © 2006 Elsevier B.V. All rights reserved.
doi:10.1016/j.clay.2006.12.007

Table 1
Composition and physical properties of the starting powders

Raw material	S_s (m^2/g)	d_{50} (μm)	ρ (g/cm^3)	Chemical composition (%)										
				SiO_2	Al_2O_3	MgO	CaO	Na_2O	K_2O	Fe_2O_3	TiO_2	MnO	P_2O_5	LOI
Kaolin CM	8.0	9.5	2.58	46.68	38.66	0.15	0.04	0.06	0.71	0.44	0.05	0.01	0.08	13.12
Talc CM	20.6	10.2	2.76	64.69	0.58	28.65	0.55	0.01	0.01	0.21	0.01	0.01	0.03	5.25
Alumina A1000 SG	10.2	0.6	3.89	0.01	99.84	0.03	0.04	0.06	–	0.02	–	–	–	–
Alumina CL 3000FG	0.7	5.2	3.89	0.01	99.8	0.002	0.03	0.05	–	0.02	–	–	–	–

The production of cordierite can be done directly by mixing (Yalamaç and Akkurt, 2006):

1) single compounds like oxides, hydroxides, and carbonates;
2) double compounds, like clays, talc, sepiolite, forsterite, enstatite, etc., and
3) triple compounds like chlorite.

The most frequent mixtures are the following:

- Clay + Talc + (Al_2O_3 or SiO_2),
- Clay + $Mg(OH)_2$ + Additives,
- Clay + Talc + Gibbsite (Tamborenea et al., 2004; Yalamaç and Akkurt, 2006),
- Talc + Diatomite + Al_2O_3 (Goren et al., 2006).
- Talc + Kaolin + SiO_2 + Feldspar (Acimovic et al., 2003),
- Kaolin + Quartz + Sepiolite (Acimovic et al., 2003),
- Talc + Kaolin + SiO_2 + Al_2O_3(Gonzàlez-Velasco et al., 1999),
- Magnesium compounds+kaolinite (Kobayashi et al., 2000),
- Alkaline-earth aluminosilicate glass + Kaolin + Al_2O_3 + Magnesite (Tulgayanov et al., 2002),
- Talc + Calcined alumina + Fly ash (Kumar et al., 2000),
- Talc + Kaolin + MgO (Yamuna et al., 2004).

One of the problems derived from the use of natural raw materials is their coarse particle size that limits the reactivity. Many studies have been done to evaluate the effects of grinding on clay minerals, including kaolinite and talc (Aglietti, 1994; Sánchez-Soto et al., 1997; Tamborenea et al., 2004; Zbik and Smart, 2005; Yalamaç and Akkurt, 2006). These studies conclude that intense mechano-chemical effects occur during grinding, leading to the destruction of the laminar structure of those substances and hence, amorphization takes place. There is a critical grinding time from which a reaggregation process among particles starts through adhesion forces. Grinding increases the reactivity of powders via particle size reduction, which increases the specific surface area so that sintering temperature may be reduced. The synthesis temperature of cordierite has been successfully reduced by combined effect of additives and intensive grinding (Yalamaç and Akkurt, 2006).

In spite of the broad body of work focusing synthesis and characterization of cordierite powders by solid state reaction of oxides, and the effect of grinding, the studies concerning the surface chemistry of those mixtures and the rheological behaviour of concentrated suspensions are scarce. One possible reason for this is the complex surface chemistry of kaolin and talc, with a large pH-dependency in terms of dissolution and surface potential, which is related to the laminar structure of silicates. As a consequence of the highly layered arrangement the preparation of concentrated slips with high packing fraction is difficult. Some studies concerning the surface behaviour and rheology of talc suspensions have been reported recently (Zbik and Smart, 2002; Bremmell and Addai-Mensah, 2005; Yao et al., 2005).

Cordierite-based materials have been shaped by slip casting using concentrated aqueous suspensions of commercial cordierite powders (Camerucci et al.,

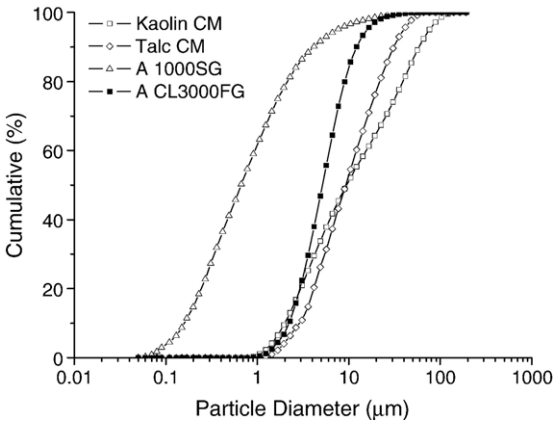

Fig. 1. Cumulative curves of particle size distributions of starting powders.

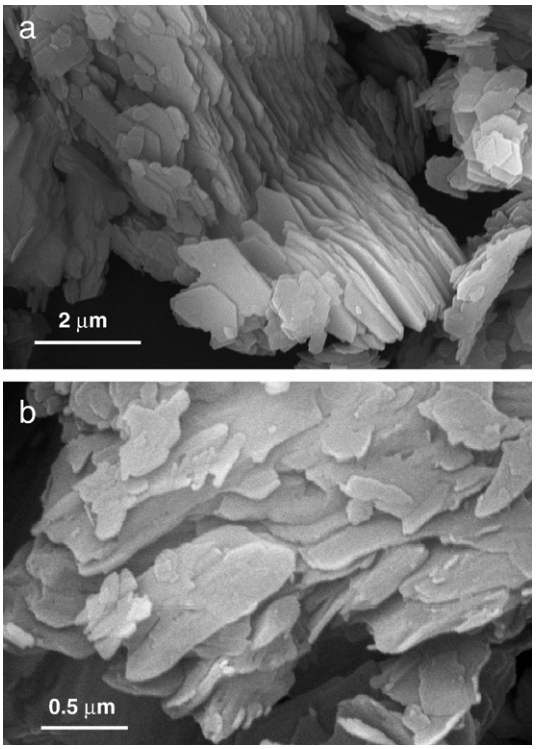

Fig. 2. FEM micrographs showing the platelet-like morphology of as-received kaolin (a) and talc (b) powders.

1998). Cordierite-based glass-ceramics have been also obtained from powders prepared by mixing Al_2O_3, $Mg(NO_3)_2{\cdot}6H_2O$ and SiO_2 to which an earth-alkaline borosilicate glass was added to reduce sintering temperature (Mei et al., 2001, 2006).

This work deals with the synthesis of cordierite materials from kaolin/talc/alumina suspensions. Concentrated suspensions have been prepared and optimized by controlling the rheological behavior as a function of the nature and concentration of deflocculant, pH, particle size of alumina, ageing time, etc. Once the mixture was optimized and talc-rich compositions could be prepared to low viscosity, the slip casting performance was studied. Preliminary sintering studies were carried out in order to determine the thermal conditions needed to promote the formation of the cordierite phase. Finally, cordierite foams were obtained from the optimized slip by the replica method using polyurethane foam.

2. Experimental

The composition of the cordierite phase consists of SiO_2/Al_2O_3/MgO in molar ratios 55.6/22.2/22.2 (weight ratios being 51.4/34.9/13.8). To promote the formation of this phase the following starting powders were used in this work: kaolin and talc (both provided by Colorminas S.A., Criciúma, Brazil and alumina (1000SG and CL3000FG, both from Alcoa, USA). These compounds were mixed in relative weight contents of 40.0 wt.% kaolin, 43.8 wt.% talc and 16.2 wt.% alumina. The characteristics of these powders are shown in Table 1. Fig. 1 plots the particle size distribution of the starting powders.

Particle size distributions were measured by laser diffraction using a Mastersizer S apparatus (Malvern, UK). Morphology of the starting powders was observed by field-emission microscopy, FEM (Hitachi S-4700 type I, Japan). Alumina particles are more or less spherical with a small aspect ratio, quite different to those of talc and kaolin, which have the typical platelet-like shape and a lamellar structure, where a card-pack agglomeration is favoured. Fig. 2 shows general FEM pictures of the as-received kaolin and talc particles. The face-to-face agglomeration is also responsible for the coarse particle size distribution measured by the laser diffraction technique, where a spherical equivalent diameter is finally evaluated and thus, subjected to a relatively large error.

Aqueous suspensions were prepared by mixing the powders in the proportions given above. Homogenization was carried out using a high shear mixer for 3 min (Silverson L2R, UK), although some tests were performed using mechanical helices agitation or ball milling for comparison purposes. Optimization of the suspensions was studied for a constant solids loading of 40 vol.% and changing other dispersion parameters, such as deflocculant type and content, ageing time, particle size of alumina, pH, etc.

The following commercial deflocculants were tested: sodium hexametaphosphate, calgon (Carlo Erba, Italy), and three synthetic polyelectrolytes, a polyphosphate (Giessfix G3), and two polyacrylic-based deflocculants, Dolapix PCN and Dolapix CE64, the last being an alkaline-free polyacrylate. All three were supplied by Zschimmer–Schwarz (Germany).

To study the stability in water zeta potential measurements were performed for suspensions of each powder at optimum dispersing conditions, i.e. with 1.5 wt.% Dolapix PCN. To

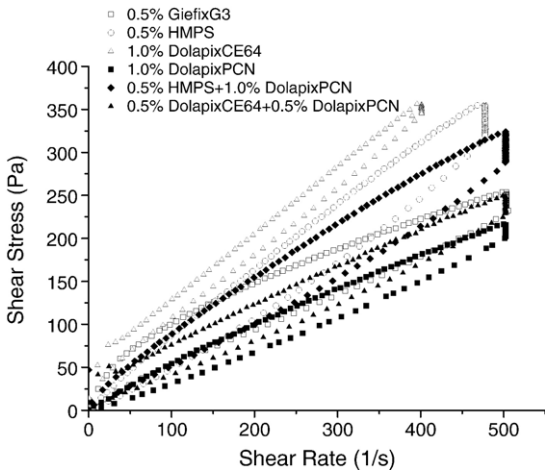

Fig. 3. Flow curves of slips prepared to 40 vol.% solids with different deflocculants.

Table 2
Rheological parameters of 40 vol.% slips with different types of deflocculant

Deflocculant (wt.%)	A (kPa/s)	τ_0 (Pa)	η_{500} (mPa.s)
0.5% GiesfixG3	28.3	0.38	506
0.5% HMPS	42.8	–	753
1.0% Dolapix CE64	40.5	3.04	899
1.0% Dolapix PCN	20.9	0.34	433
0.5% HMPS+1.0% Dolapix PCN	27.0	2.72	650
0.5% Dolapix CE64+0.5% Dolapix PCN	31.3	1.72	500

allow improved stabilization pH was varied between 7 and 11 using HCl 10^{-1} N and KOH 10^{-1} N. Measurements were performed using a microelectrophoresis technique (Zetameter 3.0+, USA).

The rheological behaviour was studied using a rotational rheometer (RS50, Haake, Thermo Electron Co., USA) with a double-cone/plate sensor configuration (DC60/2°, Haake). Flow curves were obtained at controlled rate conditions (CR) with a three-stage measuring program with a linear increase of shear rate from 0 to 1000 s^{-1} in 180 s, a plateau at 1000 s^{-1} for 60 s, and a further decrease to zero shear rate in 180 s. Thixotropy was calculated as the area enclosed between the up-curve and the down-curve in the controlled rate flow curves for the measuring conditions described above.

Rheological measurements were also performed at controlled stress conditions (CS) in order to evaluate better the behaviour in the low shear region. The yield stress values were calculated from the CS measurements as the intercepting point of two straight lines with different slope in the log–log plot of strain versus stress.

To study the sintering conditions dense ceramic pieces were first obtained by slip casting on plaster of Paris moulds. Cast green densities were determined by Archimedes' method in mercury after drying for 48 h at room temperature. Dynamic sintering studies were performed with a differential dilatometer (Setsys 16/18, Setaram, France). Sintered densities were measured by immersion in mercury. Evolution of phases was accomplished by differential thermal analysis (DTA) and thermogravimetry (TG) using a STA 409 equipment (Netzsch, Germany). X-ray diffraction (D5000, Siemens, Germany) was used to determine the crystalline phases using ground materials. Microstructure of the sintered pieces was observed by optical microscopy (Carl Zeiss, Germany) on polished and thermally etched surfaces.

Table 3
Rheological parameters of 40 vol.% slips as a function of concentration of deflocculant (Dolapix PCN)

Deflocculant (wt.%)	A (kPa/s)	τ_0 (Pa)	η_{500} (mPa.s)
0.75%	30.1	0.79	524
1.0%	20.9	0.34	433
1.5%	9.9	0.37	312
2.0%	18.8	0.36	404

Once the sintering conditions were defined for the dense bodies the porous materials were prepared by the replica method by impregnation with the slip of a polymer foam. After consolidation of the porous structures they were sintered at those conditions selected for dense, slip cast bodies (1350 °C/1 h) and observed by optical microscopy.

3. Results and discussion

Rheological studies were first performed using a variety of commercial deflocculants in order to select that one leading to lower viscosity of the mixture. Homogenization was performed using different procedures (helices agitator, ball mill and high shear mixer), the best results being obtained for the high shear mixer. The CR flow curves of 40 vol.% slips prepared with different deflocculants are plotted in Fig. 3 for a maximum shear rate of 500 s^{-1}. The values of thixotropy (A) and yield stress τ_0 of these suspensions

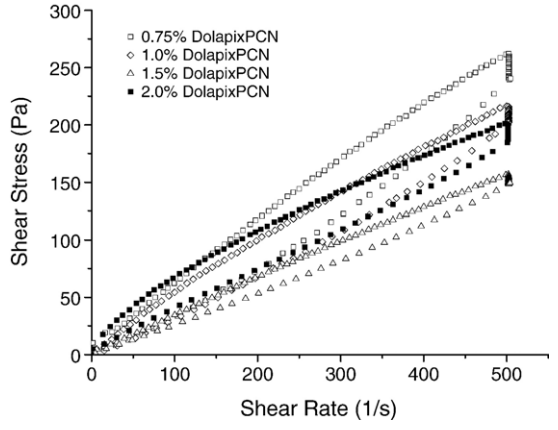

Fig. 4. Flow curves of slips prepared to 40 vol.% solids with different concentrations of the deflocculant Dolapix PCN.

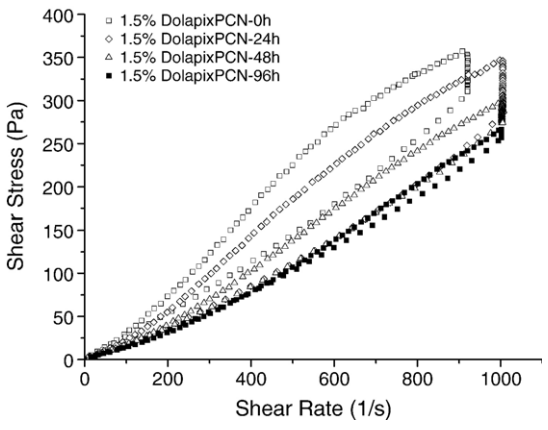

Fig. 5. Effect of ageing time on the flow curves of slips prepared to 40 vol.% solids with 1.5 wt.% of Dolapix PCN.

Table 4
Rheological parameters of 40 vol.% slips with 1.5 wt.% Dolapix PCN at different ageing times

Ageing time (h)	A (kPa/s)	τ_0 (Pa)	η_{500} (mPa.s)
0	101.3	0.36	450
24	65.6	0.39	371
48	25.2	0.46	276
96	7.2	0.33	215

are shown in Table 2, and confirm previous statements. The viscosity (η) and the thixotropy are lower for the deflocculant Dolapix PCN, so we select this one for further studies.

The effect of the concentration of this dispersant can be seen in the flow curves of Fig. 4. The lowest viscosity and thixotropy are measured for slips containing 1.5 wt.% Dolapix PCN, as confirmed by the rheological parameters summarized in Table 3. Hence, all further experiments were performed using 40 vol.% slips dispersed with 1.5 wt.% Dolapix PCN.

An important concern for industrial applications is to evaluate the stability of the slip against ageing time. The CR flow curves corresponding to the as-prepared slip and after ageing times of 24, 48 and 96 h are plotted in Fig. 5. It is clearly observed that viscosity decreases for increasing ageing times, as well as the thixotropic cycle, which is significantly reduced after 96 h ageing. This means that the structure of the slip is continuously changing with time until a better equilibrium condition is reached after a few days, this being probably related to the slow adsorption of the polyelectrolyte that tends to separate the plate-like particles. Table 4 summarizes the rheological parameters of the selected slip at different ageing times.

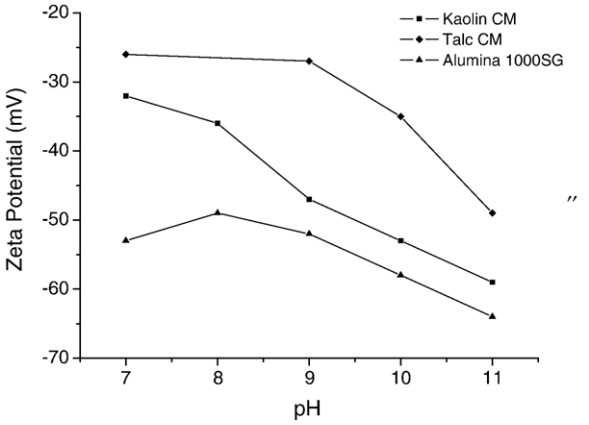

Fig. 7. Variation of zeta potential with pH for diluted suspensions of the starting powders containing 1.5 wt.% of Dolapix PCN.

In order to reduce the viscosity of the mixtures two parameters were changed, the size distribution of alumina powders and the final pH of the slip. On one hand, the particle size distribution of alumina was changed by adding a second powder of alumina with coarser particle size (Alcoa CL3000FG, USA, with a mean particle size of 5.7 μm). Fig. 6 shows the flow curves of the as-prepared mixture with the starting fine alumina. Two similar slips were prepared in which the alumina was replaced by a mixture of the two alumina powders, coarse and fine, in two relative ratios 15/85 and 85/15, respectively. In all cases, slips were maintained at their natural pH (by 8.3). When replacing 15% of the starting alumina powder by a coarser fraction the viscosity tends to decrease although a broad thixotropic cycle is still present. So, bimodality of alumina reduces a little the viscosity but does not change the thixotropy. The flow curve of the lower viscosity slip

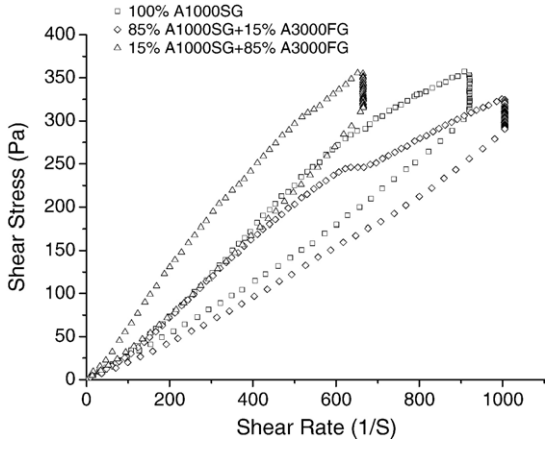

Fig. 6. Flow curves of slips prepared to 40 vol.% solids with the coarse alumina and with coarse/fine ratios of 85/15 and 15/85.

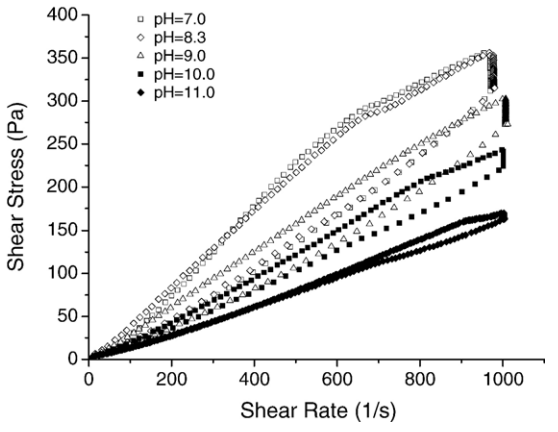

Fig. 8. Flow curves of slips prepared to 40 vol.% solids with 1.5 wt.% of Dolapix PCN at different pH values.

Table 5
Rheological parameters of 40 vol.% slips with 1.5 wt.% Dolapix PCN with pHs ranging from 7 to 11

pH	A (kPa/s)	τ_0 (Pa)	η_{500} (mPa.s)
7.0	69.8	0.41	459
8.3	93.8	0.35	433
9.0	38.1	0.36	315
10.0	17.7	0.36	243
11.0	4.8	0.35	159

Table 6
Green densities of slip cast bodies prepared at different pH

pH	ρ (g/cm^3) (±0.03)	ρ (% TD) (±0.5%)
7	1.62	57.5
8.3	1.63	58.1
9	1.63	58.1
10	1.65	58.5
11	1.66	59.0

was measured after 90 h ageing, and the flow curve overlapped with that of the fresh slip, so that these dispersing conditions assure that stability is preserved for a few days. Considering the beneficial effect of using a bimodal mixture of alumina, this 15/85 coarse/fine mixture was then maintained in the subsequent part of the work.

On the other hand, the effect of pH on the slip stability was studied by measuring the zeta potential of diluted suspensions and the flow behaviour of concentrated slips. For such measurements the optimized mixtures with 15% coarse alumina were used. Zeta potentials were measured for suspensions prepared to pH values of 7, 8.3 (natural pH), 9, 10, and 11. The rheological behaviour was measured for slips prepared at the same pH values. All suspensions contained 1.5 wt. % polyelectrolyte.

Fig. 7 shows the variation of zeta potential of the starting powders as a function of pH, measured in the alkaline region. All three powders give negative zeta potential at any pH, as expected since all of them contain polyelectrolyte, and the absolute values are always higher than 25 mV, which is considered the minimum zeta potential required to produce stable slips. The effect of anionic polyelectrolytes on alumina or kaolin is very well known, the isoelectric point shifts towards lower pH, thus increasing the stability at the considered pH values. For a given pH the zeta potential increases (becomes more negative) from talc to kaolin and to alumina, which has the highest stability, this being related to the lower particle size and its more spherical shape.

CR flow curves measured up to 1000 s^{-1} of slips with pHs ranging from 7 to 11 are plotted in Fig. 8 and the corresponding rheological parameters are summarized in Table 5. Comparing with flow curves obtained at different processing conditions (Figs. 5 and 6), it can be demonstrated that it is the pH the parameter controlling the rheology of the mixtures rather than the particle size, since both the viscosity and the thixotropy decrease as pH increases. The effect of ageing time on the rheological behavior of the mixtures at pH 11 is plotted in Fig. 9, which shows that stability is maintained with time. Hence, low viscosity slips without any ageing effect within 3 days are obtained when replacing 15% of alumina powder by a coarser fraction and maintaining a pH value of 11.

The green densities of dry slip cast bodies were found to be very similar although there was a very slight tendency to increase with the pH of the suspensions, as it can be seen in Table 6. This small variation is also

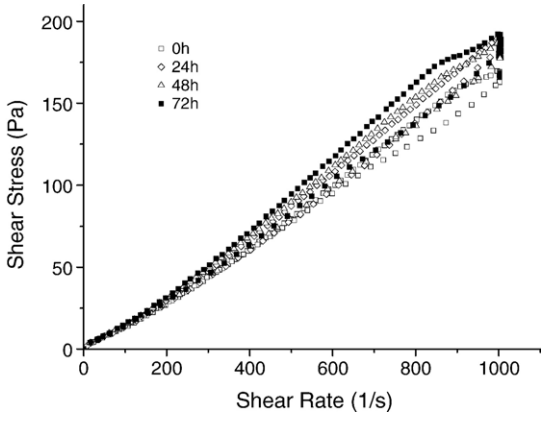

Fig. 9. Effect of ageing time on the flow curves of slips prepared to 40 vol.% solids at pH 11 with 1.5 wt.% of Dolapix PCN.

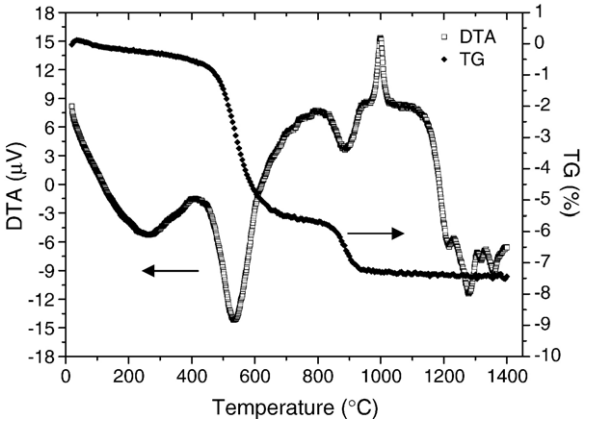

Fig. 10. DTA/TG curves of slip cast green bodies treated up to 1400 °C.

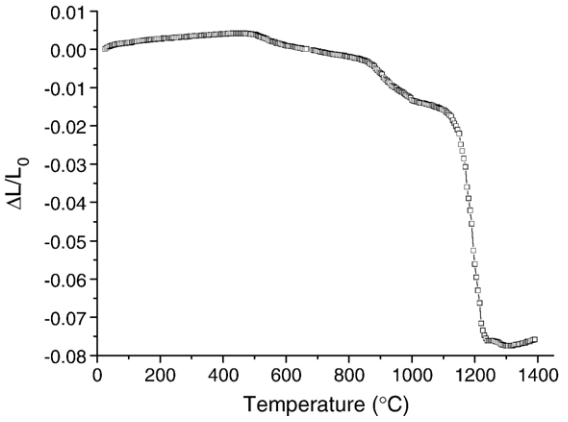

Fig. 11. Dilatometric curve of slip cast green bodies treated up to 1400 °C.

explained considering that all other processing parameters have been previously optimized.

Green samples were subjected to dynamic sintering studies and differential thermal analysis (DTA) and thermogravimetry (TG). Fig. 10 plots the DTA/TG results. It can be seen that there is a broad endothermic peak at temperatures ranging from 200 °C to 300 °C corresponding to the loss of adsorbed water. At 550 °C there is a sharp endothermic peak corresponding to the dehydroxylation of kaolin, and a shoulder is also appreciated in the TG curve. A smaller endothermic peak in the DTA curve centred at 885 °C can be assigned to the dehydroxylation of talc to promote the formation of enstatite. This behaviour is also appreciated in the TG curve that shows a weight loss in this region. At nearly 1000 °C an exothermic sharp peak is recorded that corresponds to the transformation of the non-crystalline structure of the kaolinite into a premullite phase. This transformation occurs without any change of mass. The endothermic peak appearing above 1100 °C is related to the formation of liquid phase that cannot be easily identified. Within the range 1200–1350 °C a series of three weak peaks appear, centred at 1230, 1305, and 1335 °C, respectively. Similar results were found by de Aza and Espinosa de los Monteros (1972), which assigned the first one to transformation of premullite into mullite and the other two to the formation of cordierite. Tamborenea et al. (2004) only detected the two last peaks associated to cordierite formation.

Fig. 11 plots the results of the dilatometric analysis, showing that small shrinkage effects are recorded at those temperatures corresponding to the endothermic peaks observed in the DTA curve as discussed above. The larger densification rate occurs at 1190 °C, this behaviour being related to the formation of a glassy phase, as demonstrated by the large peak starting at this temperature in the DTA curve. Densification occurs before the cordierite phase has been formed, as expected for a reaction sintering process. Recrystallization of glassy phase into cordierite phase inhibits the liquid phase sintering process so that no more densification takes place from that point.

The previous statements were confirmed through XRD analysis. Fig. 12 plots the XRD patterns of

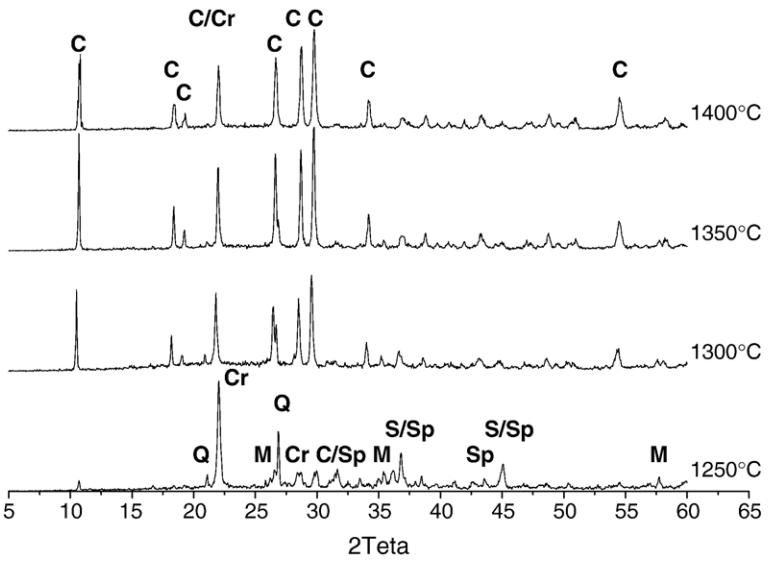

Fig. 12. XRD of slip cast green bodies treated at different temperatures for 1 h. C) Cordierite, Cr) Cristobalite, M) Mullite, S) Spinel, Sp) Sapphirine, Q) Quartz.

Table 7
Apparent densities of slip cast bodies sintered at different temperatures

Temperature (°C)	ρ (g/cm^3), (±0.03)
1250	2.13
1300	2.21
1350	2.22
1400	2.18

samples treated at temperatures ranging from 1250° to 1400 °C, taken every 50 °C. It can be seen that at 1250 °C the major components of the mixture are silica (present as both quartz and cristobalite phases), sapphirine, spinel and some mullite, also. When temperature rises to 1300 °C the cordierite phase appears as the main phase in the XRD pattern, although a very small shoulder corresponding to quartz is still present. Similar spectra are obtained when temperature is further increased, with cordierite as main phase but without the quartz peak.

The evolution of the apparent density of slip cast samples is presented in Table 7 as a function of sintering temperature. It can be seen that there is a density increase between 1250° and 1300 °C, in good agreement with the change of phases revealed by the XRD spectra. The density seems to apparently decrease from 1350 °C, this being probably related to the evolution of phases and pores. Fig. 13 shows a general view of the microstructure observed by optical microscopy of samples treated at the same temperatures. From this series of pictures it can be seen that the number of pores decreases as temperature increases, although pore size largely increases. At 1250 °C some large grains of quartz can be still detected, that disappear at higher temperatures, in agreement with XRD patterns. No significant changes are observed between the microstructure of samples treated at 1350° and 1400 °C, so that the tendency of the density to decrease must be related to the larger content of the cordierite phase, which has lower density.

As observed in pictures of Fig. 13 a high remaining porosity is maintained in all cases. The porosity of these slip cast samples would be reduced by milling the starting powders to lower particle sizes. Since the final objective of the present work was to obtain porous bodies by the replica method there was no milling.

Once the slip was optimized from a rheological perspective and the thermal treatment necessary to promote the formation of cordierite was established, the porous bodies were produced by the replica method. The sponge was immersed into the ceramic suspension until four times and then left in air to dry for 24 h. The obtained preform was subjected to a two-step thermal

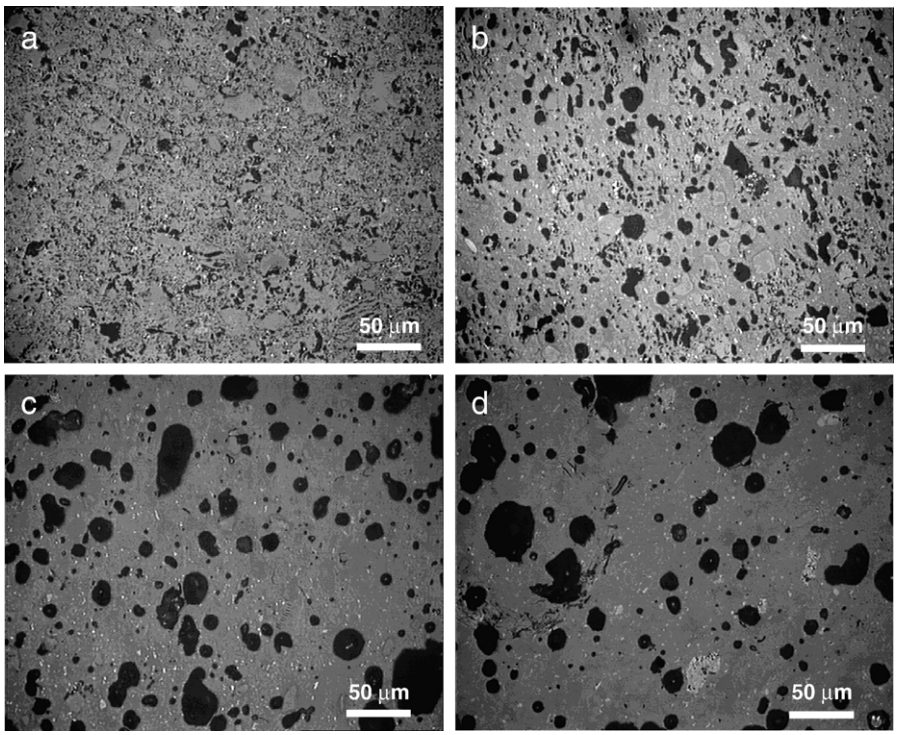

Fig. 13. Optical microscopy pictures of slip cast bodies treated at 1250 (a), 1300 (b), 1350 (c) and 1400 °C (d).

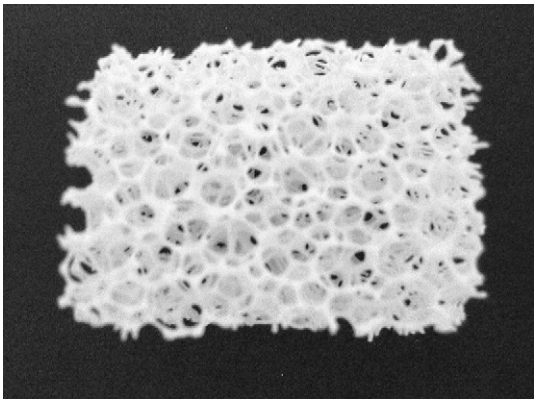

Fig. 14. Ceramic foam sintered at 1350 °C/1 h.

treatment involving a first step at 550 °C/30 min to promote the burning out of the polymer, followed by the conventional treatment for sintering at 1350 °C/1 h, selected considering the results shown above. Fig. 14 shows a picture of the sintered porous cordierite-based material. This picture demonstrates that optimization of slip rheology allows easy manufacture of cordierite films by the replica method from talc-rich suspensions.

4. Conclusions

Aqueous suspensions of kaolin/talc/alumina mixtures with relative weight ratios of 40/43.8/16.2 have been prepared to a solids loading of 40 vol.% and rheologically characterized in order to obtain the better dispersing conditions and the optimum green properties after slip casting in plaster moulds, while avoiding intermediate complex steps such as grinding/machining, which would affect significantly to the reactivity of the powders and the physical-chemistry in the system.

The rheological behaviour was characterized and optimized as a function of different processing parameters that strongly influence the dispersibility, such as mixing procedure, nature and concentration of deflocculant, pH, particle size of alumina, etc. The best rheological behaviour, i.e. the lowest viscosity, yield stress and thixotropy, were obtained for slips prepared by mechanical mixing and containing 1.5 wt.% of the commercial polyelectrolyte Dolapix PCN adjusting the pH to 11 with KOH, replacing 15 wt.% of fine alumina particles by a coarser fraction.

These slips were slip cast and the resulting green bodies led to relative densities up to 59% of theoretical value. Dynamic and static sintering tests, accomplished by XRD analysis, demonstrated that at 1250 °C quartz and cristobalite, spinel and sapphirine are the principal phases and some mullite have already been formed, but the cordierite phase only appears at 1300 °C. The microstructure reveals that samples sintered at any temperature have a large remaining porosity, as a consequence of the large particle size of the raw materials. Better densities and higher microstructural uniformity could be expected for samples obtained by using ground powders, but this is out of the scope of this work, where porous bodies are to be prepared. For such purpose the replica method was used by impregnating a polyurethane sponge into the optimized slip and treating the resulting dry body at 1350 °C/1 h with an intermediate step at 550 °C for burning out the polymer.

Acknowledgements

Dr. Rodrigues acknowledges the CNPq (Conselho Nacional Desenvolvimento Científico e Tecnológico, Brasil) for the concesión of a fellowship. Colorminas Colorifício e Mineração S.A (Criciúma, Brasil) is acknowledged for supplying kaolin and talc raw materials. This work has been supported by the Spanish Ministry of Education and Science (MEC, project MAT2003-00836).

References

Acimovic, Z., Pavlovic, L., Trumbulovic, L., Andric, L., Stamatovic, M., 2003. Synthesis and characterization of the cordierite ceramics from nonstandard raw materials for applications in foundry. Mater. Lett. 57, 2651–5266.

Aglietti, E.F., 1994. The effect of dry grinding on the structure of talc. Appl. Clay Sci. 9, 139–147.

Awano, M., Takagi, H., Kuwabara, Y., 1992. Grinding effects on the synthesis and sintering of cordierite. J. Am. Ceram. Soc. 75, 2535–2540.

Bertran, C.A., da Silva, N.T., Thim, G.P., 2000. Citric acid effect on aqueous sol–gel cordierite synthesis. J. Non-Cryst. Solids 273, 140–144.

Bremmell, K.E., Addai-Mensah, J., 2005. Interfacial-chemistry mediated behavior of colloidal talc dispersions. J. Colloid Interface Sci. 283, 385–391.

Camerucci, M.A., Cavalieri, A.L., Moreno, R., 1998. Slip casting of cordierite and cordierite–mullite materials. J. Eur. Ceram. Soc. 18, 2149–2157.

Chandran, R.G., Patil, K.C., 1993. Combustion synthesis, characterization, sintering and microstructure of cordierite. Br. Ceram., Trans. J. 92, 239–245.

de Aza, S., Espinosa de los Monteros, J., 1972. Mecanismo de la formación de cordierita en cuerpos cerámicos. Bol. Soc. Esp. Ceram. Vidr. 11, 315–321.

González-Velasco, J.R., Gutiérrez-Ortiz, M.A., Ferret, R., Aranzabal, A., Botas, J.A., 1999. Synthesis of cordierite monolithic honeycomb by solid state reaction of precursor oxides. J. Mater. Sci. 34, 1999–2002.

Goren, R., Gocmez, H., Ozgur, C., 2006. Synthesis of cordierite powder from talc, diatomite and alumina. Ceram. Int. 32, 407–409.

Knickerbocker, S.H., Kumar, A.H., Herron, L.W., 1993. Cordierite glass-ceramic for multilayer ceramic packing. Am. Ceram. Soc. Bull. 72, 90–95.

Kobayashi, Y., Sumi, K., Kato, E., 2000. Preparation of dense cordierite ceramics from magnesium compounds and kaolinite without additives. Ceram. Int. 26, 739–743.

Kumar, S., Singh, K.K., Ramachadrarao, P., 2000. Synthesis of cordierite from fly ash and its refractory properties. J. Mater. Sci. Lett. 19, 1263–1265.

Mei, S., Yang, J., Fereira, J.M.F., 2001. Cordierite-based glass-ceramics processed by slip casting. J. Eur. Ceram. Soc. 21, 185–193.

Mei, S., Yang, J., Xu, X., Quaresma, S., Agathopoulos, S., Fereira, J.M.F., 2006. Aqueous tape casting processing of low dielectric constant cordierite-based glass-ceramics—selection of a binder. J. Eur. Ceram. Soc. 26, 67–71.

Mussler, B., Shafer, M., 1984. Preparation and properties of mullite–cordierite composites. Am. Ceram. Soc. Bull. 63, 705–710.

Sánchez-Soto, P.J., Wiewióra, A., Avilés, M.A., Justo, A., Pérez-Maqueda, L.A., Pérez-Rodríguez, J.L., Bylina, P., 1997. Talc from Puebla de Lillo, Spain. II. Effect of dry grinding on particle size and shape. Appl. Clay Sci. 12, 297–312.

Tamborenea, S., Mazzoni, A.D.D., Aglietti, E.F., 2004. Mechano-chemical activation of minerals on the cordierite synthesis. Thermochim. Acta 411, 219–224.

Tulgayanov, D.U., Tukhtaev, M.E., Escalante, J.I., Ribeiro, M.J., Labrincha, J.A., 2002. Processing of cordierite based ceramics from alkaline-earth aluminosilicate glass, kaolin, alumina and magnesite. J. Eur. Ceram. Soc. 22, 1775–1782.

Yalamaç, E., Akkurt, S., 2006. Additive and intensive grinding effects on the synthesis of cordierite. Ceram. Int. 32, 825–832.

Yamuna, A., Johnson, R., Mahajan, Y.R., Lalithambika, M., 2004. Kaolin-based cordierite for pollution control. J. Eur. Ceram. Soc. 24, 65–73.

Yao, X., Tan, S., Huang, Z., Jiang, D., 2005. Dispersion of talc particles in silica sol. Mater. Lett. 59, 100–104.

Zbik, M., Smart, R.St.C., 2002. Dispersion of kaolinite and talc in aqueous solution: nano-morphology and nano-bubble entrapment. Miner. Eng. 15, 277–286.

Zbik, M., Smart, R.St.C., 2005. Influence of dry grinding on talc and kaolinite morphology: inhibition of nano-bubble formation and improved dispersion. Miner. Eng. 18, 969–976.